



Original Research Article

In-depth investigation on physicochemical and thermal properties of magnesium (II) gluconate using spectroscopic and thermoanalytical techniques



Mahendra Kumar Trivedi^a, Neena Dixit^b, Parthasarathi Panda^c, Kalyan Kumar Sethi^c, Snehasis Jana^{c,*}

^a Trivedi Global, Inc., Henderson 89052, Nevada, USA

^b National Institute of Technology, Raipur 492010, Chhattisgarh, India

^c Trivedi Science Research Laboratory Pvt. Ltd., Bhopal 462026, Madhya Pradesh, India

ARTICLE INFO

Keywords:

Magnesium gluconate
Solid state properties
Particle size analysis
Thermal analysis
Spectroscopic analysis

ABSTRACT

Magnesium gluconate is a classical organometallic pharmaceutical compound used for the prevention and treatment of hypomagnesemia as a source of magnesium ion. The present research described the in-depth study on solid state properties *viz.* physicochemical and thermal properties of magnesium gluconate using sophisticated analytical techniques like Powder X-ray diffraction (PXRD), particle size analysis (PSA), Fourier transform infrared (FT-IR) spectrometry, ultraviolet–visible (UV–Vis) spectroscopy, thermogravimetric analysis (TGA)/differential thermogravimetric analysis (DTG), and differential scanning calorimetry (DSC). Magnesium gluconate was found to be crystalline in nature along with the crystallite size ranging from 14.10 to 47.35 nm. The particle size distribution was at $d(0.1)=6.552\ \mu\text{m}$, $d(0.5)=38.299\ \mu\text{m}$, $d(0.9)=173.712\ \mu\text{m}$ and $D(4,3)=67.122\ \mu\text{m}$ along with the specific surface area of $0.372\ \text{m}^2/\text{g}$. The wavelength for the maximum absorbance was at 198.0 nm. Magnesium gluconate exhibited 88.51% weight loss with three stages of thermal degradation process up to 895.18 °C from room temperature. The TGA/DTG thermograms of the analyte indicated that magnesium gluconate was thermally stable up to around 165 °C. Consequently, the melting temperature of magnesium gluconate was found to be 169.90 °C along with the enthalpy of fusion of 308.7 J/g. Thus, the authors conclude that the achieved results from this study are very useful in pharmaceutical and nutraceutical industries for the identification, characterization and qualitative analysis of magnesium gluconate for preformulation studies and also for developing magnesium gluconate based novel formulation.

1. Introduction

Magnesium gluconate ($\text{MgC}_{12}\text{H}_{22}\text{O}_{14}$) is an organometallic pharmaceutical salt of magnesium with gluconic acid, which is a weak organic acid formed from glucose through a simple dehydrogenation reaction catalyzed by glucose oxidase [1]. Magnesium gluconate has the potential industrial application in nutraceutical and pharmaceutical sectors as a source of magnesium ion (Mg^{2+}), which is the major essential nutrient for human body functions, such as structural constituent of bone, regulator of more than 300 enzymes, cofactor for DNA and RNA synthesis, reproduction and protein synthesis [2–4]. There are several factors responsible for magnesium deficiency or hypomagnesemia in our body [5,6]. Magnesium is effective for the prevention and treatment of numerous ailments such as cardiovascular diseases [7], diabetes mellitus [8], pre-eclampsia and

eclampsia, Alzheimer's disease, asthma, and hearing loss [9–11]. Magnesium gluconate can be used as potent antioxidant for the prevention and treatment of many diseases, such as diabetes mellitus, allergy, inflammatory diseases, immunological disorders [12,13], ischemia/reperfusion injury [14] along with other antioxidant agents. It can be used as an oral tocolytic agent [15], neuroprotective agent [16], and also in the skin-tightening cosmetic composition [17]. Furthermore, magnesium gluconate shows the highest bioavailability of magnesium and is also a physiologically acceptable salt among the other commercially available magnesium salts [13,18].

Pharmaceutical solids during process, development and storage have a common tendency to exist in more than one form or crystal structure, *i.e.* polymorphism, which shows different physicochemical and thermal properties including melting point, solubility, dissolution rate, physical/

Peer review under responsibility of Xi'an Jiaotong University.

* Corresponding author.

E-mail address: jana@trivedisrl.com (S. Jana).

<http://dx.doi.org/10.1016/j.jpha.2017.03.006>

Received 31 August 2016; Received in revised form 14 March 2017; Accepted 22 March 2017

Available online 22 March 2017

2095-1779/ © 2017 Xi'an Jiaotong University. Production and hosting by Elsevier B.V. This is an open access article under the CC BY-NC-ND license (<http://creativecommons.org/licenses/by-nc-nd/4.0/>).

chemical stability, mechanical, optical properties, etc. [19,20]. Selection of the optimum solid form of the pharmaceuticals/nutraceuticals plays an important role in the successful drug product performance, viz. processing, solubility, dissolution rate, therapeutic efficacy, toxicity, bioavailability, and stability with respect to the atmospheric conditions and formulation excipients [20,21]. Powder X-ray diffraction (PXRD), particle size analysis (PSA), Fourier transform infrared (FT-IR) spectrometry, ultraviolet–visible (UV–Vis) spectroscopy, differential scanning calorimetry (DSC), thermogravimetric analysis (TGA), and differential thermogravimetric analysis (DTG) are advanced analytical techniques used for the solid state characterization of the pharmaceutical solids and also helpful in elucidating various difficulties faced during their formulation and development [19–23]. To the best of our knowledge, a comprehensive characterization on physicochemical and thermal properties of magnesium gluconate using PXRD, PSA, FT-IR, UV–Vis spectroscopy, TGA, DTG and DSC techniques has not been reported till to date. Therefore, PXRD, PSA, FT-IR, UV–Vis spectroscopy, TGA, DTG and DSC techniques were conducted in this study to analyze the solid state properties, viz. physicochemical and thermal properties of magnesium gluconate.

2. Experimental

2.1. Chemicals

Magnesium gluconate hydrate was purchased from Tokyo Chemical Industry Co., Ltd. (TCI), Japan. All the other chemicals used in this experiment were of analytical grade procured from the vendors in India.

2.2. PXRD analysis

The XRD patterns of solid state form of magnesium gluconate were measured with PANalytical X'Pert Pro powder X-ray diffractometer, UK. Radiations were produced from CuK α source and filtered through nickel filters with a wavelength of 0.154 nm, running at 45 kV voltage and 40 mA current. Scanning was done at a scanning rate of 0.2089°/s over a 2θ range from 2° to 50° at a step size of 0.017° and step time of 10.16 s. The ratio of K α -2 and K α -1 in this instrument was 0.5 (k, equipment constant). The XRD data were collected in the form of the Bragg angle ($^{\circ}2\theta$) vs. intensity (counts per second), and a detailed table containing information on peak intensity counts, d value (Å), relative intensity (%), full width half maximum (FWHM) ($^{\circ}2\theta$), area (cts $^{\circ}2\theta$) using X'Pert data collector and X'Pert high score plus processing software. The crystallite size (G) was calculated from the Scherrer equation [24,25] as follows:

$$G = k\lambda / (b \cos\theta) \quad (1)$$

where k is the equipment constant (0.5), λ is the X-ray wavelength (0.154 nm); b in radians is the full-width at half of the peaks and θ is the corresponding Bragg angle.

2.3. PSA

PSA was conducted on Malvern Mastersizer 2000 (UK) with a detection range between 0.01 and 3000 μm using wet method. The sample unit (Hydro 2000 SM) was filled with a dispersant medium (Sunflower oil) and the stirrer was operated at 2500 rpm. Refractive index values for dispersant and samples were 0.0 and 1.46, respectively. After the background measurement followed by alignment of the optics, the sample was added into the sample unit with constant monitoring the obscuration and the addition of sample was stopped when the obscuration reached between 10% and 20%. When the obscuration was stable, the measurement was taken twice and the average histogram was recorded. Consequently, PSA of magnesium gluconate was repeated for six times to obtain the average particle size distribution. d(0.1) μm , d(0.5) μm , and d(0.9) μm represent particle

diameter corresponding to 10%, 50%, and 90% of the cumulative distribution. D(4,3) represents the average mass-volume diameter and the specific surface area (SSA) (m^2/g) was calculated by using software Mastersizer 2000.

2.4. FT-IR spectroscopy analysis

FT-IR analysis was performed on Spectrum two (Perkin Elmer, USA) Fourier transform infrared spectrometer with the frequency range of 400–4000 cm^{-1} at a resolution of 4 by mixing magnesium gluconate with potassium bromide (KBr). FT-IR reveals the information about functional groups present in magnesium gluconate.

2.5. UV–Vis spectroscopy analysis

The UV–Vis analysis was carried out using Shimadzu UV-2450 with UV Probe, Japan. The spectrum was recorded using 1 cm quartz cell that has a slit width of 1.0 nm. The wavelength range chosen for recording the spectrum was 190–800 nm. The wavelength of the absorbance maximum (λ_{max}) was recorded.

2.6. TGA/DTG

TGA/DTG thermograms of magnesium gluconate were obtained in a TGA Q50 thermoanalyzer apparatus, USA under dynamic nitrogen atmosphere (50 mL/min) using a platinum crucible at a heating rate of 10 $^{\circ}\text{C}/\text{min}$ from room temperature to 900 $^{\circ}\text{C}$ with a sample mass of 7.58 mg. In TGA, the weight loss for each step was recorded in gram as well as in percent loss with respect to the initial weight. In DTG, the onset, endset, and peak temperature of each peak were recorded.

2.7. DSC

DSC curve of magnesium gluconate was accomplished in a DSC Q20 differential scanning calorimeter, USA under dynamic nitrogen atmosphere (50 mL/min) with a sample mass of 8.23 mg using aluminum pan at a heating rate of 10 $^{\circ}\text{C}/\text{min}$ from 25 to 450 $^{\circ}\text{C}$. The value for onset, endset, peak temperature, peak height (mJ or mW), peak area, and change in heat (J/g) for each peak were recorded.

3. Results and discussion

3.1. PXRD analysis

PXRD is an accurate and reliable technique for the identification and characterization of polymorph, monitoring of the stability, method development and validation for qualitative as well as quantitative analysis of pharmaceuticals/nutraceuticals in pharmaceutical and nutraceutical industries [23].

Crystal pattern and crystallite size of a pharmaceutical salt play an important role on its solubility, dissolution, and bioavailability [26]. Besides, the changes of the PXRD patterns such as crystallite size and relative intensities indicate the modification of the morphology of the crystal and are commonly used to identify and characterize the different polymorphic transition of a pharmaceutical solid compound [27,28]. Thus, PXRD study was conducted to explore the crystalline pattern of magnesium gluconate.

The PXRD diffractogram of magnesium gluconate (Fig. 1) exhibited the well-defined, narrow, sharp and intense peaks at 2θ equal to nearly 5.235°, 10.050°, 14.059°, 15.996°, 16.562°, 18.108°, 18.644°, 19.226°, 20.258°, 21.091°, 22.551°, 23.764°, 24.913°, 25.662°, 27.526°, 29.520°, 30.785°, 31.591°, 32.099°, 34.004°, 34.657°, 35.886°, 37.769°, 39.789°, 40.596°, 41.998°, 42.700°, 44.308°, 45.464°, and 49.451°. These results indicated that the sample was crystalline in nature. Besides, other XRD parameters such as relative intensity (%), full width half maximum (FWHM), area, and crystallite size (G, nm) for

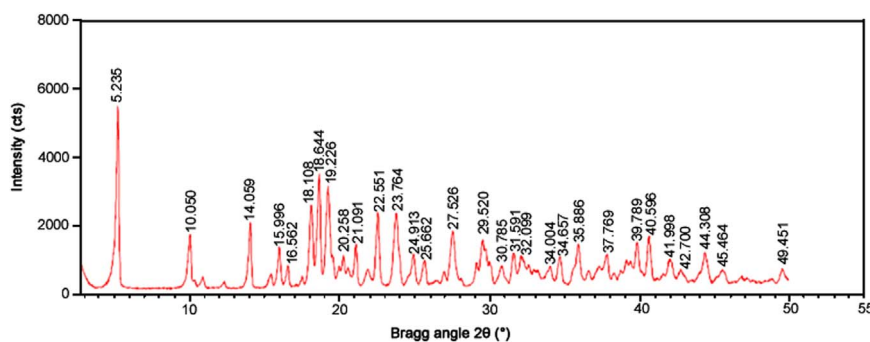


Fig. 1. Powder X-ray diffraction pattern of magnesium gluconate.

Table 1

Powder X-ray diffraction data with Bragg angle, d-spacing, relative intensities, FWHM, areas, and crystallite size of magnesium gluconate.

Bragg angle (°2θ)	d-spacing (Å)	Rel. Int. ^a (%)	FWHM ^b (°2θ)	Area (cts*°2θ)	Crystallite size (G, nm)
5.235	16.883	100.00	0.1171	618.06	37.63
10.050	8.801	29.40	0.1840	285.53	24.01
14.059	6.300	35.85	0.1506	284.85	29.45
15.996	5.541	21.65	0.1338	152.89	33.22
16.562	5.353	12.26	0.1506	97.43	29.53
18.108	4.899	45.42	0.1338	320.81	33.31
18.644	4.759	62.70	0.2342	775.04	19.05
19.226	4.617	55.20	0.2007	584.81	22.24
20.258	4.383	17.95	0.1506	142.63	29.69
21.091	4.212	24.14	0.1673	213.13	26.76
22.551	3.943	40.94	0.1506	325.32	29.80
23.764	3.744	40.94	0.2007	433.79	22.41
24.913	3.574	18.88	0.1338	133.35	33.69
25.662	3.471	15.26	0.1673	134.76	26.99
27.526	3.241	30.99	0.1673	273.64	27.09
29.520	3.026	26.46	0.1338	186.90	34.02
30.785	2.904	12.03	0.2676	169.98	17.06
31.591	2.832	18.65	0.2007	197.56	22.80
32.099	2.789	17.46	0.1673	154.15	27.38
34.004	2.637	11.80	0.1338	83.33	34.41
34.657	2.588	17.43	0.2175	200.03	21.20
35.886	2.502	24.11	0.1673	212.86	27.66
37.769	2.382	18.12	0.2007	191.97	23.18
39.789	2.266	24.50	0.2175	281.17	24.50
40.596	2.222	28.22	0.1673	249.13	28.06
41.988	2.151	15.83	0.3346	279.61	14.10
42.700	2.118	9.96	0.2676	140.68	17.67
44.308	2.044	18.77	0.1004	99.45	47.35
45.464	1.993	9.65	0.2040	140.48	23.40
49.451	1.842	10.78	0.1224	94.09	39.61

^a Relative intensity.

^b Full width at half maximum.

magnesium gluconate are presented in Table 1. The crystallite size was calculated according to the Eq. (1) and found to be in the range from 14.10 to 47.35 nm (Table 1).

3.2. PSA

The particle properties like particle size, shape and surface area of the active pharmaceutical ingredients are very important for successful dosage form design and drug performance, viz. solubility, dissolution and *in vivo* bioavailability [29].

So, measurement of particle size distribution is a key requirement during the process and development of the products in pharmaceutical and nutraceutical industries. Here, PSA of magnesium gluconate was repeated for six times and the results are summarized in Table 2. The average particle size distribution of magnesium gluconate ($n=6$) was observed at $d(0.1)=6.552 \mu\text{m}$, $d(0.5)=38.299 \mu\text{m}$, $d(0.9)=173.712 \mu\text{m}$

Table 2

Particle size distribution of magnesium gluconate.

Measurement	d (0.1) (μm)	d (0.5) (μm)	d (0.9) (μm)	D (4,3) (μm)	SSA (m ² /g)
1	6.970	38.511	182.415	70.172	0.359
2	6.070	33.495	148.380	57.845	0.403
3	6.567	40.582	173.282	67.754	0.361
4	6.687	38.070	161.290	63.454	0.367
5	6.306	36.480	173.810	65.508	0.385
6	6.712	42.656	203.094	77.999	0.354
Average	6.552	38.299	173.712	67.122	0.372

$d(0.1)$, $d(0.5)$, and $d(0.9)$: particle diameter corresponding to 10%, 50%, and 90% of the cumulative distribution, $D(4,3)$: the average mass-volume diameter, and SSA: the specific surface area.

and $D(4,3)=67.122 \mu\text{m}$. The average SSA of magnesium gluconate was $0.372 \text{ m}^2/\text{g}$.

3.3. FT-IR spectroscopy analysis

The FT-IR spectroscopy has been applied for evaluating the alterations in molecular conformations, crystal packing and hydrogen bonding arrangements for various solid state forms of the pharmaceutical solids [30]. The FT-IR spectrum of magnesium gluconate (Fig. 2) exhibited only one broad band of high intensity in the range from 3200 to 3600 cm^{-1} with centroid at 3399 cm^{-1} that is due to the stretching vibration of hydroxyl group of water present in magnesium gluconate hydrate.

The stretching vibrations bands for the primary and secondary hydroxyl groups from the gluconate part of magnesium gluconate appeared in the range of 3200 – 3600 cm^{-1} , which was not observed due to the intensive broad band of water [31]. Consequently, the deformation vibration bands at 1434 cm^{-1} as well as 636 and 577 cm^{-1} were observed in the spectrum of magnesium gluconate for the primary and secondary hydroxyl groups in the plane $\delta(\text{OH})$ and out-of-plane $\gamma(\text{OH})$, respectively. The spectrum also displayed C-H stretching at 2935 and 1381 cm^{-1} . A very sharp and intensive vibration band at 1606 cm^{-1} for C=O stretching was observed in the spectrum, indicating the presence of carbonyl group in magnesium gluconate (Fig. 2). Thereafter, the C-O stretching vibration band for the primary alcohol group was found at 1057 cm^{-1} . Consequently, the absorption peaks at 1229 and 1142 cm^{-1} due to the C-O stretching vibrations of the secondary alcohol groups were also observed in the spectrum of magnesium gluconate. Thus, FT-IR analysis revealed the presence of the characteristic absorption bands for the functional groups present in the structure of magnesium gluconate (Fig. 3).

3.4. UV-Vis spectroscopy analysis

Literature reported that the 0.1% aqueous solution of magnesium gluconate showed a maximum absorption peak (λ_{max}) at 194.7 nm [32]. The UV-Vis spectrum of our sample (Fig. 4) showed that the maximum absorbance peak (λ_{max}) was at 198.0 nm .

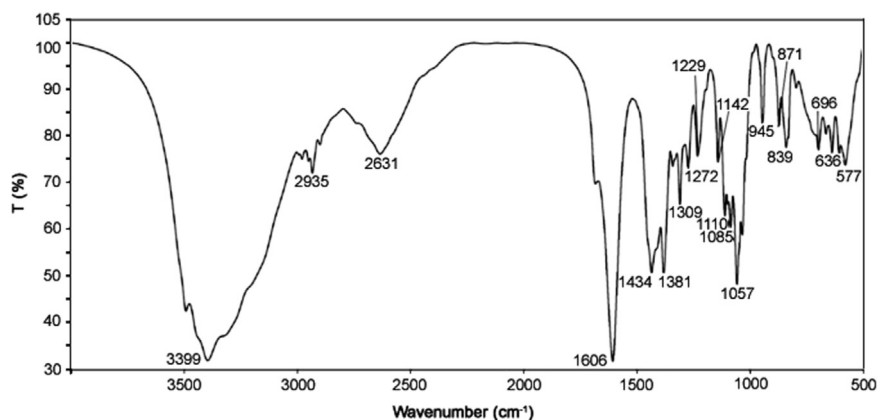


Fig. 2. FT-IR spectrum of magnesium gluconate.

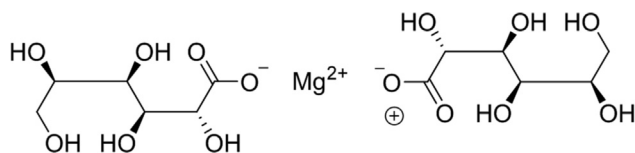


Fig. 3. Structure of magnesium gluconate.

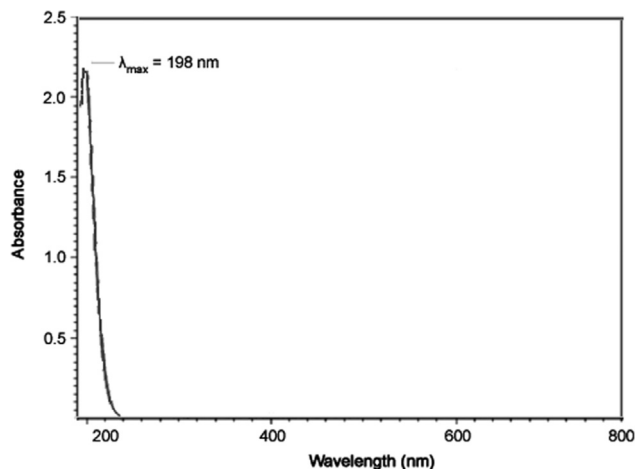


Fig. 4. UV-Vis spectrum of magnesium (II) gluconate.

UV absorbance of magnesium gluconate occurs due to the $\sigma \rightarrow \sigma^*$ energy transition by σ -bonded electrons present in the C-C and C-H functional groups and $\pi \rightarrow \pi^*$ transition due to the presence of lone pair

electrons in C=O group. These types of electronic transitions occurred when the difference in energy between the lowest unoccupied molecular orbital and the highest occupied molecular orbital is significantly higher than the activation energy of the compound [33]. This UV-Vis data can be used for identification and quantitative analysis of magnesium gluconate in pharmaceutical and nutraceutical industries.

3.5. Thermal analysis

The stability of a pharmaceutical/nutraceutical solid ingredient with respect to the atmospheric conditions plays an important role in the hydrate formation upon processing, formulation, storage and packaging. The thermoanalytical techniques such as TGA/DTG and DSC are widely used for the assessment and/or comparison of the thermal stabilities of pharmaceutical solids, determination of several kinetic parameters like activation energy, and reaction order, and achievement of drug/excipient compatibility data for the pre-formulation study. The TGA/DTG analysis identifies all types of thermal reactions in terms of variations in mass, while the DSC detects reactions that may or may not be related to the weight loss, such as physical phenomena (fusion) [34]. Labuschagne [35] reported that magnesium gluconate exhibited a mass loss of 5.8% at 177 °C from the TGA/DSC analysis of magnesium gluconate at a scan rate of 10 °C/min under air. In this study, TGA and DSC analyses were performed at a scan rate of 10 °C/min under nitrogen atmosphere.

3.5.1. TGA/DTG

The TGA thermogram of magnesium gluconate (Fig. 5A) revealed the three steps of thermal decomposition (Table 3).

At 142.35 °C, magnesium gluconate exhibited a mass loss of only 2.42%, which is due to water removal from magnesium gluconate

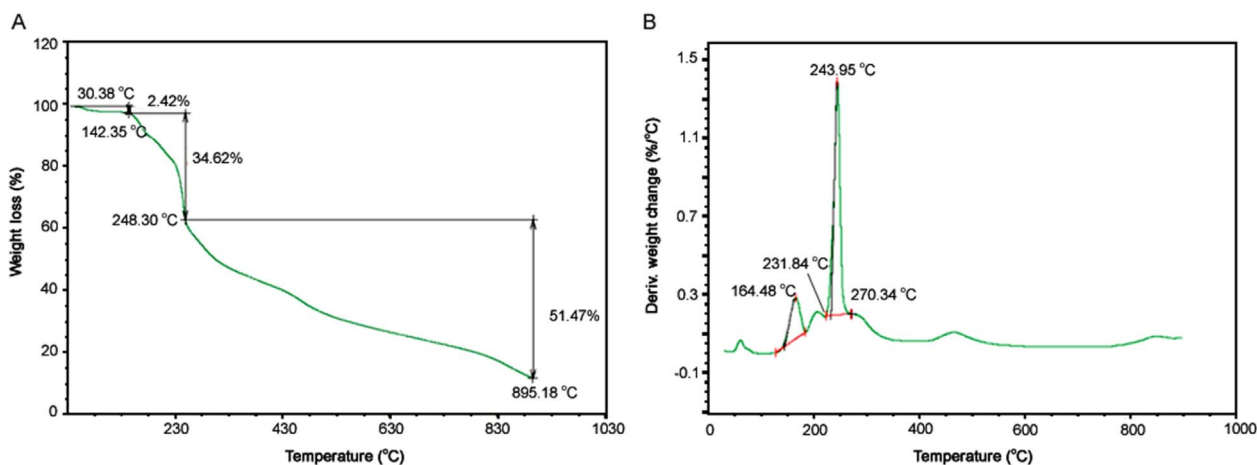


Fig. 5. (A) TGA thermogram and (B) DTG thermogram of magnesium gluconate.

Table 3
Thermal degradation analysis of magnesium gluconate.

Steps of degradation	Temperature (°C)	% Weight loss
1	30.38–142.35	2.42
2	142.35–248.30	34.62
3	248.30–895.18	51.47

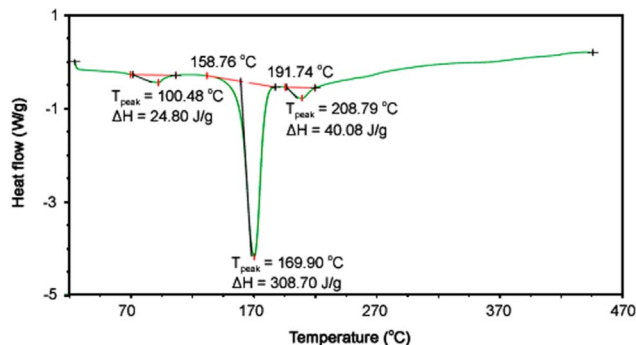


Fig. 6. DSC thermogram of magnesium gluconate.

hydrate. Consequently, the second thermal degradation of magnesium gluconate occurred with a high rate of mass loss (34.62%) due to the decomposition of the hydroxyl groups and carbonyl groups of the gluconate portion. After that, magnesium gluconate exhibited the gradual mass loss of 51.47% up to 895.18 °C and the carbon oxidation occurred at the last step of degradation. Magnesium gluconate showed 88.51% weight loss from 30.38 to 895.18 °C. The DTG thermogram of magnesium gluconate (Fig. 5B) exhibited that the sample displayed two peaks at 164.48 and 243.95 °C. The onset and endset temperatures of the major peak were at 231.84 and 270.34 °C, respectively. The TGA/DTG thermograms of the analyte (Fig. 5) indicated that magnesium gluconate was thermally stable up to around 165 °C.

3.5.2. DSC analysis

The DSC thermogram of magnesium gluconate (Fig. 6) exhibited the presence of a sharp endothermic inflection at 169.90 °C along with a broad endothermic peak at 100.48 °C.

The broad peak at 100.48 °C might be due to the vaporization temperature for removal of water present inside magnesium gluconate hydrate. The enthalpy of vaporization of this compound is found to be 24.80 J/g. The peak temperature at 169.90 °C is the melting temperature of magnesium gluconate having the enthalpy of fusion (ΔH_{fusion}) of 308.70 J/g.

4. Conclusions

The present study successfully explored the physicochemical and thermal properties of a classical pharmaceutical/nutraceutical compound like magnesium gluconate in details using PXRD, PSA, FT-IR, UV-Vis, TGA, DTG and DSC techniques. In summary, magnesium gluconate was found to be crystalline in nature having crystallite size from 14.10 to 47.35 nm, maximum absorbance peak at 198.0 nm, and thermally stable up to around 165 °C with a melting temperature at 169.90 °C having enthalpy of fusion of 308.7 J/g. The acquired data are very useful in identifying and characterizing magnesium gluconate from its various polymorphs. Therefore, pharmaceutical and nutraceutical industries might require these pieces of information for the identification, characterization and qualitative analysis of magnesium gluconate for preformulation studies and also for developing magnesium gluconate-based novel formulation. This study might enhance the readers' interest in knowing more about the solid state properties of organometallic pharmaceutical solids like magnesium gluconate.

Conflicts of interest

The authors declare that there are no conflicts of interest.

Acknowledgments

The authors are highly grateful to GVK Biosciences Pvt. Ltd., Hyderabad, India, for their assistance and support during this work.

References

- [1] S. Ramachandran, P. Fontanille, A. Pandey, et al., Gluconic acid: properties, applications and microbial production, *Food Technol. Biotechnol.* 44 (2006) 185–195.
- [2] M.K. Choi, C.M. Weaver, Daily intake of magnesium and its relation to urinary excretion in Korean healthy adults consuming self-selected diets, *Biol. Trace Elem. Res.* 176 (2017) 105–113.
- [3] R. Ponka, E. Fokou, E. Beaucher, et al., Nutrient content of some Cameroonian traditional dishes and their potential contribution to dietary reference intakes, *Food Sci. Nutr.* 4 (2016) 696–705.
- [4] N.J. Birch, Magnesium in biology and medicine: an overview in *Metal ions in biological systems*, H. Sigel, A. Sigel (Eds.), *Compendium on Magnesium and its Role in Biology, Nutrition and Physiology* Vol. 26, Marcel Dekker Inc, New York, 1990: 105–115.
- [5] J.H. William, J. Danziger, Magnesium deficiency and proton-pump inhibitor use: a clinical review, *J. Clin. Pharmacol.* 56 (2016) 660–668.
- [6] R. Swaminathan, Magnesium metabolism and its disorders, *Clin. Biochem. Rev.* 24 (2003) 47–66.
- [7] J.G. Gums, Magnesium in cardiovascular and other disorders, *Am. J. Health Syst. Pharm.* 61 (2004) 1569–1576.
- [8] C.H. Sales, Lde F. Pedrosa, Magnesium and diabetes mellitus: their relation, *Clin. Nutr.* 25 (2006) 554–562.
- [9] M.P. Guerrero, S.L. Volpe, J.J. Mao, Therapeutic uses of magnesium, *Am. Fam. Physician* 80 (2009) 157–162.
- [10] B.I. Nageris, D. Ulanovski, J. Attias, Magnesium treatment for sudden hearing loss, *Ann. Otol. Rhinol. Laryngol.* 113 (2004) 672–675.
- [11] U. Gröber, J. Schmidt, K. Kisters, Magnesium in prevention and therapy, *Nutrients* 7 (2015) 8199–8226.
- [12] T.E. Fleming, H.C. Mansmann Jr., Methods and compositions for the prevention and treatment of diabetes mellitus, United States Patent 5871769, 1999.
- [13] T.E. Fleming, H.C. Mansmann Jr., Methods and compositions for the prevention and treatment of immunological disorders, inflammatory diseases and infections, United States Patent 5939394, 1999.
- [14] W.B. Weglicki, Intravenous magnesium gluconate for treatment of conditions caused by excessive oxidative stress due to free radical distribution, United States Patent 6100297, 2000.
- [15] R.W. Martin, J.N. Martin Jr, J.A. Pryor, et al., Comparison of oral ritodrine and magnesium gluconate for ambulatory tocolysis, *Am. J. Obstet. Gynecol.* 158 (1988) 1440–1445.
- [16] R.J. Turner, K.W. Dasilva, C. O'Connor, et al., Magnesium gluconate offers no more protection than magnesium sulphate following diffuse traumatic brain injury in rats, *J. Am. Coll. Nutr.* 23 (2004) 541S–544S.
- [17] K.H. Lee, S.H. Chung, J.H. Song, et al., Cosmetic compositions for skin-tightening and method of skin-tightening using the same, United States Patent 8580741 B2, 2013.
- [18] C. Coudray, M. Rambeau, C. Feillet-Coudray, et al., Study of magnesium bioavailability from ten organic and inorganic Mg salts in Mg-depleted rats using a stable isotope approach, *Magnes. Res.* 18 (2005) 215–223.
- [19] H.G. Brittain, *Polymorphism in Pharmaceutical Solids in Drugs and Pharmaceutical Sciences*, 2nd ed. Vol. 192, Informa Healthcare USA, Inc., New York, 2009.
- [20] K.R. Gupta, S.S. Askarkar, R.R. Joshi, et al., Solid state properties: preparation and characterization, *Der Pharm. Sin.* 6 (2015) 45–64.
- [21] R.A. Storey, I. Ymen, *Solid State Characterization of Pharmaceuticals*, Wiley-Blackwell, UK, 2011.
- [22] P. Guerrieri, A.C.F. Rumondor, T. Li, et al., Analysis of relationships between solid-state properties, counterion, and developability of pharmaceutical salts, *AAPS PharmSciTech* 11 (2010) 1212–1222.
- [23] A. Chauhan, P. Chauhan, Powder XRD technique and its applications in science and technology, *J. Anal. Bioanal. Tech.* 5 (2014) 212.
- [24] L. Alexander, H.P. Klug, Determination of crystallite size with the X-Ray spectrometer, *J. Appl. Phys.* 21 (1950) 137.
- [25] J.I. Langford, A.J.C. Wilson, Scherrer after sixty years: a survey and some new results in the determination of crystallite size, *J. Appl. Cryst.* 11 (1978) 102–113.
- [26] N. Blagden, M. de Matas, P.T. Gavan, et al., Crystal engineering of active pharmaceutical ingredients to improve solubility and dissolution rates, *Adv. Drug Deliv. Rev.* 59 (2007) 617–630.
- [27] M. Inoue, I. Hirasawa, The relationship between crystal morphology and XRD peak intensity on $\text{CaSO}_4 \cdot 2\text{H}_2\text{O}$, *J. Cryst. Growth* 380 (2013) 169–175.

- [28] K. Raza, P. Kumar, S. Ratan, et al., Polymorphism: the phenomenon affecting the performance of drugs, *SOJ Pharm. Pharm. Sci.* 1 (2014) 1–10.
- [29] P. Khadka, J. Ro, H. Kim, et al., Pharmaceutical particle technologies: an approach to improve drug solubility, dissolution and bioavailability, *Asian J. Pharm. Sci.* 9 (2014) 304–316.
- [30] G. Chawla, P. Gupta, R. Thilagavathi, et al., Characterization of solid-state forms of celecoxib, *Eur. J. Pharm. Sci.* 20 (2003) 305–317.
- [31] V.D. Nikolic, D.P. Ilic, L.B. Nikolic, et al., The synthesis and characterization of iron (II) gluconate, *Adv. Technol.* 3 (2014) 16–24.
- [32] L. Ji, W. Yin, M. Fu-Jia, Confirmation of the chemical structure of magnesium gluconate, *Pharm. Care Res.* 4 (2004) 272–273.
- [33] M. Hesse, H. Meier, B. Zeeh, *Spectroscopic Methods in Organic Chemistry*, Georg Thieme Verlag Stuttgart, New York, 1997.
- [34] R. Alves, T.V.S. Reis, L.C.C. Silva, et al., Thermal behavior and decomposition kinetics of rifampicin polymorphs under isothermal and non-isothermal conditions, *Braz. J. Pharm. Sci.* 46 (2010) 343–351.
- [35] F.J.W.J. Labuschagne, *Metal Catalysed Intumescence of Polyhydroxyl Compounds*, University of Pretoria, 2003.